Static magnetic properties of the many-sublattice antiferromagnet $Ca_2Fe_2O_5$

P. Marchukov,* R. Geick, and C. Brotzeller
Physical Institute of the University, 8700 Würzburg, Germany

W. Treutmann
Mineralogy Institute of the University, 3550 Marburg, Germany

E. G. Rudashevsky
General Physics Institute of the Academy of Sciences, 117942, Moscow, Russia

A. M. Balbashov
Power Engineering Institute, 105835, Moscow, Russia

(Received 2 November 1992; revised manuscript received 30 June 1993)

We have studied the magnetization of the antiferromagnet dicalcium ferrite $Ca_2Fe_2O_5$ in magnetic fields up to 5.5 T and in the temperature range 5–330 K. Temperature dependences of the weak ferromagnetic moment m_0 and susceptibilities along the main crystallographic axes have been measured. Effective intrinsic parameters, such as an exchange field and the Dzyaloshinskiy-Moriya field have been obtained as a function of temperature. Possible magnetic structures have been analyzed by means of comprehensive group-theoretical consideration and a phenomenological free energy has been derived. Problems involving hedgehog structure, parallel susceptibility, field-induced spin reorientation, magnitude of the Dzyaloshinskiy-Moriya interaction, and the origin of the weak ferromagnetism are also discussed. It is shown that $Ca_2Fe_2O_5$ can be described as two canted antiferromagnets putting one into another with an *antiferromagnetic* interaction between the weak ferromagnetic components.

I. INTRODUCTION

Interest in antiferromagnets has shifted in recent years from simple two-sublattice structures to more complicated many-sublattice systems. Such systems display a variety of effects and also offer the possibility to verify models for simple antiferromagnets within an investigation of many-sublattice antiferromagnets. From this point of view, dicalcium ferrite, $Ca_2Fe_2O_5$ (Ref. 1), is a very suitable object for investigation. Since it has eight Fe ions per unit cell, a general description must involve eight sublattices. The magnetic structure of $Ca_2Fe_2O_5$ was studied by means of the Mössbauer effect[2–7] and neutron diffraction.[8,9] It has been shown that dicalcium ferrite is an antiferromagnet with a sufficiently high Néel temperature, $T_N = 725$ K,[4,10] and a complicated magnetic structure. The presence of a weak ferromagnetic moment[9–12] makes this substance even more interesting.

In spite of many previous experimental studies of the magnetic structure, there has been no detailed theoretical analysis of the spin arrangement in $Ca_2Fe_2O_5$. It is obvious that eight sublattices can form many different magnetic configurations. This would be useful for the prediction and interpretation of experimental results. We shall try to determine possible magnetic structures in $Ca_2Fe_2O_5$, using group-theoretical considerations which involve symmetry arguments only. Following Turov and Najsh[13] we shall analyze the spin arrangement of dicalcium ferrite. The advantage of this method is that it yields all conceivable magnetic structures allowed by symmetry. In addition, the corresponding free energy can be constructed in a very general form which includes all possible interactions, such that we do not neglect any term regardless of its actual value in nature. The experimental aspect of this work was motivated, in part, by the absence of detailed magnetization measurements on $Ca_2Fe_2O_5$ and, in particular, the absence of reliable measurements of the weak ferromagnetic component in this substance. Note that between the early suggestion of weak ferromagnetism in $Ca_2Fe_2O_5$ by Hirone[11] and the recent measurements of that by Nagata and Ohta,[12] almost two decades have elapsed. However, in the latter investigation the spontaneous ferromagnetic component m_0 was obtained only at room temperature. Neither the temperature dependence of m_0 nor that of the susceptibilities along the crystallographic axes nor the Dzyaloshinskiy-Moriya field[14] (responsible for the ferromagnetic moment in the antiferromagnets) have been measured until now.

In Sec. III of the paper we interpret the experimental results by means of the phenomenological free energy obtained from group-theoretical considerations. Some attendant problems such as hedgehog structure, parallel susceptibility, field-induced spin reorientation, value of the Dzyaloshinskiy-Moriya interaction, and origin of the weak ferromagnetism are also discussed.

II. GROUP-THEORETICAL ANALYSIS

The crystal structure of dicalcium ferrite was determined by Bertaut, Blum, and Sagnieres[1] and belongs to

the orthorhombic space group *Pcmn* (D_{2h}^{16}) [the lattice parameters, $a=5.598$, $b=14.769$, and $c=5.425$ Å (Ref. 15)]. There are four molecules and consequently, eight Fe ions per unit cell that are equally distributed between two different symmetry sites (I and m) in two corresponding sets of layers parallel to the ac plane which alternate along the b axis. Fe(1) ions (octahedral coordination) are on the fourfold symmetry positions ($4a$), (000, $\frac{1}{2}0\frac{1}{2}$, $0\frac{1}{2}0$, $\frac{1}{2}\frac{1}{2}\frac{1}{2}$) and will be numbered 1,2,3,4. These sites are centers of inversion. Fe(2) ions (tetrahedral coordination) are on the $4c$ positions, $\pm(x,\frac{1}{4},z;\frac{1}{2}-x,\frac{1}{4},\frac{1}{2}+z)$ and will be numbered 5,6,7,8 (Fig. 1). The parameters x and z are quite small ($x=-0.066a, z=-0.054c$) and their values are magnified appreciably in Fig. 1 for clarity.

The *Pcmn* group has eight symmetry operations:[16] identity E, inversion I, three screw axes: $\tilde{C}_{2x}=(C_{2x}|\frac{1}{2}00)$, $\tilde{C}_{2y}=(C_{2y}|0\frac{1}{2}0)$, $\tilde{C}_{2z}=(C_{2x}|00\frac{1}{2})$, and three mirror-screw planes: $\tilde{\sigma}_x=(\sigma_x|00\frac{1}{2})$, $\tilde{\sigma}_y|000)$, $\tilde{\sigma}_z=(\sigma_z|\frac{1}{2}\frac{1}{2}0)$. The first symbol in each parentheses originates from the point-group symmetry operator (where C_2 is a twofold axis and σ is a mirror plane) and the second one corresponds to the translation vector inherent in a given space group. Figure 2 shows how the Fe ions transform under these symmetry operations. For instance, $\tilde{C}_{2x}$ sends 1 to 2, 3 to 4, 5 to 8, and 6 to 7. Inversion does not change the Fe(1) ions but does transform the Fe(2) ions, i.e., sends 5 to 7, 6 to 8, and so on.

The spins vectors $\mathbf{S}_i (i=1\cdots 8)$ are transformed in a complicated way under these symmetry operations. One can say, that the spins form the basis of a reducible representation. It is more reasonable (Dzyaloshinskiy[14]) to use linear combinations of the spins (so-called base vectors) which form the basis of an irreducible representation. It

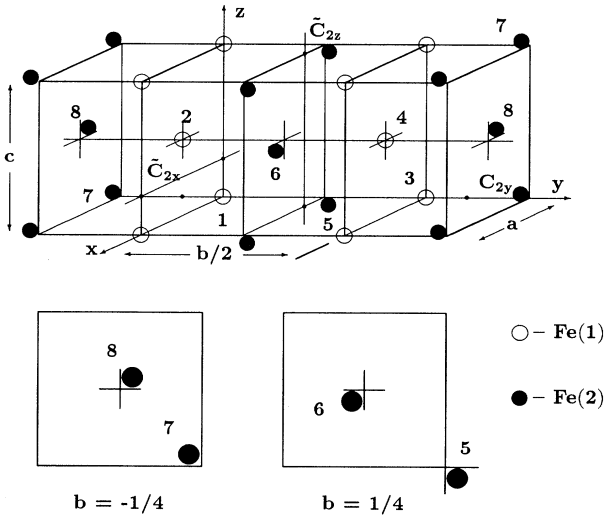

FIG. 1. Orthorhombic structure of $Ca_2Fe_2O_5$, showing only the magnetic nonequivalent Fe(1) and Fe(2) ions with octahedral (●) and tehedral (●) coordination, respectively. Insets below represent relative location of the Fe(2) ions $5\cdots 8$ in the planes $(x,\frac{1}{4},z)$ and $(x,-\frac{1}{4},z)$. From the symmetry elements only screw axes $\tilde{C}_{2j} (j=x,y,z)$ are shown.

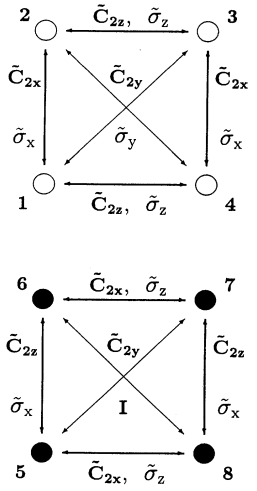

FIG. 2. Transformation properties of the Fe ions under the symmetry operations.

is clear that for the two nonequivalent sites there exist two independent sets of base vectors. It is also obvious that the simple vector sums of the spins,

$$\mathbf{m}_1=\mathbf{S}_1+\mathbf{S}_2+\mathbf{S}_3+\mathbf{S}_4 \quad \text{Fe(1)},$$

$$\mathbf{m}_2=\mathbf{S}_5+\mathbf{S}_6+\mathbf{S}_7+\mathbf{S}_8 \quad \text{Fe(2)},$$

are two of these base vectors. Other combinations which are easily found by inspection are as follows:

$$\left.\begin{aligned} \mathbf{l}_1&=\mathbf{S}_1-\mathbf{S}_2+\mathbf{S}_3-\mathbf{S}_4\\ \mathbf{a}_1&=\mathbf{S}_1-\mathbf{S}_2-\mathbf{S}_3+\mathbf{S}_4\\ \mathbf{c}_1&=\mathbf{S}_1+\mathbf{S}_2-\mathbf{S}_3-\mathbf{S}_4 \end{aligned}\right\} \text{Fe(1)},$$

$$\left.\begin{aligned} \mathbf{l}_2&=\mathbf{S}_5-\mathbf{S}_6+\mathbf{S}_7-\mathbf{S}_8\\ \mathbf{a}_2&=\mathbf{S}_5-\mathbf{S}_6-\mathbf{S}_7+\mathbf{S}_8\\ \mathbf{c}_2&=\mathbf{S}_5+\mathbf{S}_6-\mathbf{S}_7-\mathbf{S}_8 \end{aligned}\right\} \text{Fe(2)}.$$

There are eight irreducible representations for the *Pcmn* group.[17] We have listed in Table I the transformation properties of the base vector components, i.e., we show to which irreducible representation of the paramagnetic space group *Pcmn* they belong.

Each of the representations in Table I may become totally symmetric in the magnetically ordered state below

TABLE I. Irreducible representations of the group D_{2h}.

$\Gamma_i(\bar{C}_{2x}\bar{C}_{2y}I)$	m_1	l_1	a_1	c_1	m_2	l_2	a_2	c_2	Magn. Gr.
$\Gamma_1^+(+++)$		l_{1y}	a_{1z}	c_{1x}		l_{2y}			*Pcmn*
$\Gamma_2^+(-++)$	m_{1y}		a_{1x}	c_{1z}	m_{2y}				*Pc'mn'*
$\Gamma_3^+(--+)$	m_{1z}	l_{1x}		c_{1y}	m_{2z}	l_{2x}			*Pc'm'n*
$\Gamma_4^+(+-+)$	m_{1x}	l_{1z}	a_{1y}		m_{2x}	l_{2z}			*Pcm'n'*
$\Gamma_1^-(++-)$							a_{2x}	c_{2z}	
$\Gamma_2^-(-+-)$							a_{2z}	c_{2x}	
$\Gamma_3^-(---)$							a_{2y}		
$\Gamma_4^-(+--)$								c_{2y}	

the transition temperature, with the corresponding nonvanishing components of the base vectors. The resulting magnetic structures (magnetic space groups) are listed in the last column of Table I, where the apostrophe indicates that the corresponding symmetry operation has to be combined with time reversal. Thus, possible magnetic structures can be described by the symbols $\Gamma_i^{\pm}$ and are determined by nonzero components of the base vectors belonging to a given representation.

For further analysis of the magnetic configurations we must refer to the available experimental results. As was mentioned above, $Ca_2Fe_2O_5$ has a layer structure. There are only two possibilities for dicalcium ferrite to be an antiferromagnet. For the first, each layer has a ferromagnetic order with a maximum value for the $\mathbf{m}_i$ $(i=1,2)$ vectors (so-called m structure, since vector $\mathbf{m}$ is responsible for the ferromagnetic order) and an antiferromagnetic interaction between layers, i.e., $\mathbf{m}_1$ is antiparallel to $\mathbf{m}_2$. For the second, the two layers are both antiferromagnetic.

In the former configuration the spins $\mathbf{S}_1,\mathbf{S}_2,\mathbf{S}_3,\mathbf{S}_4$ have a general direction opposite to that of the spins $\mathbf{S}_5,\mathbf{S}_6,\mathbf{S}_7,\mathbf{S}_8$. In the latter configuration the antiferromagnetic structure for the Fe(2) ions can be described only by l components (l structure, $\mathbf{S}_5\|\mathbf{S}_7$, and $\mathbf{S}_6\|\mathbf{S}_8$), while the antiferromagnetic order for the Fe(1) ions could be realized either with the l structure ($\mathbf{S}_1,\mathbf{S}_3$ are opposite to $\mathbf{S}_2,\mathbf{S}_4$, such that the $\boldsymbol{l}_1$ vector has a maximum value) or with an a structure ($\mathbf{S}_1,\mathbf{S}_4$ opposite to $\mathbf{S}_2,\mathbf{S}_3$, with a maximum value for the $\mathbf{a}_1$ vector). The simplest estimation on the basis of an exchange approximation shows, that $\boldsymbol{l}$ structure for Fe(1) ions is more energetically favorable than the a structure. In addition, it would be very unlikely that two alternating layers have the magnetic structures which are described by the different base vectors. So, the Fe(1) ions have also the l structure with the $\boldsymbol{l}_1$ parallel to the $\boldsymbol{l}_2$ for the ferromagnetic interaction between the layers, or $\boldsymbol{l}_1$ antiparallel to the $\boldsymbol{l}_2$ for the antiferromagnetic one.

In experiments with substituted diamagnetic Ga^{3+} and Sc^{3+} ions, it was found,[3–5,7] that both nonequivalent layers are antiferromagnetic and interaction between them is also antiferromagnetic. In the $Ca_2Fe_2O_5$ structure, Sc^{3+} ions prefer octahedral Fe(1) sites while Ga^{3+} ions prefer tetrahedral Fe(2) sites.[18] This substitution does not produce ferrimagnetism and it implies that both layer must be antiferromagnetic. Following these experimental results we conclude from our group-theoretical considerations that each layer in $Ca_2Fe_2O_5$ should be described by l structure with the spins $\mathbf{S}_1,\mathbf{S}_3,\mathbf{S}_6,\mathbf{S}_8$ trended in one direction opposite to the spins $\mathbf{S}_2,\mathbf{S}_4,\mathbf{S}_5,\mathbf{S}_7$ ($\boldsymbol{l}_1$ antiparallel to the $\boldsymbol{l}_2$).

We would like to emphasize, that the magnetic configurations derived from the group analysis are just possible spin arrangements. The values of the vectors $\mathbf{m},\mathbf{a},\mathbf{c}$, which are mixed to the main l structure are defined by natural constants and can be very small in reality. The weak ferromagnetic component observed by Nagata and Ohta[12] at room temperature can be estimated as 10^{-3} of the antiferromagnetic vector $\boldsymbol{l}$ value. To the best of our knowledge, nothing has been reported about the $\mathbf{a}$ and $\mathbf{c}$ components in dicalcium ferrite. So we suppose these vectors are of the same order of magnitude as ferromagnetic vector $\mathbf{m}$.

Possible spin configurations allowed by the symmetry in $Ca_2Fe_2O_5$ and compatible with the available experimental results are shown in Fig. 3. It is interesting to note that the Fe(1) ions with nonequivalent spins $\mathbf{S}_1,\mathbf{S}_2,\mathbf{S}_3,\mathbf{S}_4$ form a hedgehog structure which is described by three different components of the base vectors, while the Fe(2) ions have an ordinary structure described by no more than two components of the base vectors, $\mathbf{m}_2$ and $\boldsymbol{l}_2$, with two pairs of equivalent spins, i.e., $\mathbf{S}_5=\mathbf{S}_7$ and $\mathbf{S}_6=\mathbf{S}_8$. From this point of view we can consider the magnetic configuration of the Fe(1) ions as a four-sublattice structure and that of the Fe(2) ions as a two-sublattice one.

Thus, the group-theoretical analysis yields a magnetic structure with six sublattices for dicalcium ferrite. When speaking about six sublattices we mean nonequivalent ones only. It is clear that $Ca_2Fe_2O_5$ with eight magnetic ions per unit cell must be described in a very general way with eight magnetic sublattices. However, nonzero components of the base vectors $\mathbf{a}_2$ and $\mathbf{c}_2$ can be revealed in dynamic experiments only, so for a description of the static properties the number of the sublattices reduces to six.

The magnetic structure described by the $Pcmn(\Gamma_1^+)$ group [$\mathbf{S}_i$ is parallel to the b axis of the orthorhombic crystal, see Fig. 3(a)] is purely antiferromagnetic and the existence of a weak ferromagnetic moment is strictly prohibited by symmetry. The other two antiferromagnetic spin configurations, $Pc'm'n(\Gamma_3^+)$ and $Pcm'n'(\Gamma_4^+)$ [$\mathbf{S}_i$ along the a and c axis, respectively, see Figs. 3(c) and 3(d)] are, in principal, equivalent. The $Pc'mn'(\Gamma_2^+)$ structure with ferromagnetic ordered layers is shown in Fig. 3(b).

It is easily seen that direction of the spins in dicalcium ferrite uniquely determines the magnetic configuration. In accordance with the experimental data, the spins in $Ca_2Fe_2O_5$ lie along the c axis and consequently, the spin configuration corresponds to the $Pcm'n'$ [Γ_4^+, Fig. 3(d)]. The antiferromagnetic configuration $Pc'm'n$ [Γ_3^+, Fig. 3(c)] can be induced in $Ca_2Fe_2O_5$ by applying a magnetic field along the c axis. Finally, the ferromagnetic $Pc'mn'$ [Γ_2^+, Fig. 3(b)] and purely antiferromagnetic $Pcmn$ [Γ_1^+, Fig. 3(a)] structures are not realized in nature and have only theoretical interest.

Now we can proceed to construct the free energy, restricted here to second-order terms. Table I contains all the information necessary for this. Indeed, it is well known that invariants of order 2 are obtained simply by the multiplication of two base vector components which belong to the same representation. For example, representation Γ_1^+ gives ten invariants:

$$l_{1y}^2, l_{2y}^2, c_{1x}^2, a_{1z}^2, l_{1y}c_{1x}, l_{1y}a_{1z}, l_{1y}l_{2y}, c_{1x}a_{1z}, c_{1x}l_{2y}, a_{1z}l_{2y} \ .$$

There are, all together, 58 invariants of order 2 and the free energy is a linear combination of all the invariants

with coefficients which are phenomenological parameters. It is clear, however, that the interpretation of any experimental result by means of 58 different parameters is practically impossible. To reduce the number of these phenomenological constants we must confine our free energy to the most physically important interactions: (i) isotropic symmetric exchange interactions of the Heisenberg-type $J(\mathbf{S}_i \cdot \mathbf{S}_j)$ between nearest neighbors only. There are three exchange constants: B_1 and B_2 for the two layers and B_3 for the interaction between them; (ii) antisymmetric exchange interaction of the Dzyaloshinskiy-Moriya-type $D(\mathbf{S}_i \times \mathbf{S}_j)$ between nearest neighbors only. Here there are seven parameters $(D_1,\ldots,D_7)$. However, for the sake of simplicity and because of the small value of the ferromagnetic component in $Ca_2Fe_2O_5$, we neglect the interlayer interaction and deal only with four parameters $(D_1,\ldots,D_4)$; (iii) single-ion anisotropy of the type $\sum S_{i\alpha}S_{i\beta}=(i=1\cdots4,5\cdots8,\ \alpha,\beta=x,y,z)$ for nearest neighbors, with all together, eight $(K_1,\ldots,K_8)$ parameters.

Thus, the free energy, including all principal second-order terms which are allowed by symmetry and reasonably restricted to nearest-neighbor interactions, has the following form:

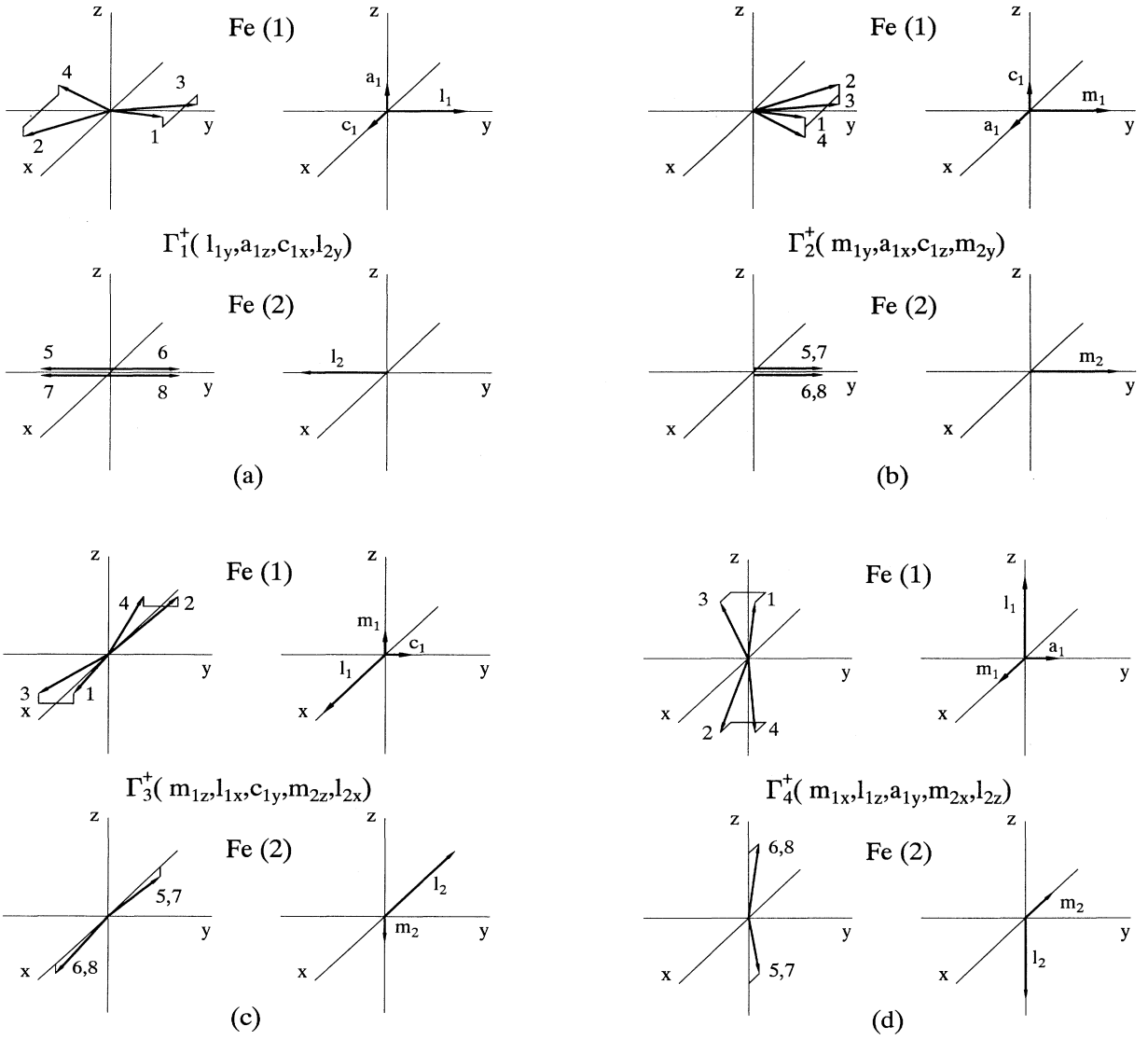

FIG. 3. Possible spin configurations in $Ca_2Fe_2O_5$. Components of the base vectors $\mathbf{m}_1$, $\mathbf{m}_2$, $\mathbf{a}_1$, and $\mathbf{c}_1$, are intentionally exaggerated. Preliminary estimation shows these vectors are 2–3 orders smaller in magnitude than antiferromagnetic vector $\boldsymbol{l}$. Ferromagnetic structure $Pc'mn'(\Gamma_2^+)$ (b) is shown in contrast to the experimental finding.

$$\Phi=\tfrac{1}{2}B_1(\mathbf{m}_1^2-\mathbf{l}_1^2-\mathbf{a}_1^2+\mathbf{c}_1^2)+\tfrac{1}{2}B_2(\mathbf{m}_2^2-\mathbf{l}_2^2-\mathbf{a}_2^2+\mathbf{c}_2^2)+B_3(\mathbf{m}_1\cdot\mathbf{m}_2+\mathbf{l}_1\cdot\mathbf{l}_2)$$
$$+D_1(m_{1y}c_{1z}+c_{1y}m_{1z}-l_{1y}a_{1z}-a_{1y}l_{1z})+D_2(m_{1z}l_{1x}+c_{1z}a_{1x}-l_{1z}m_{1x}-a_{1z}c_{1x})$$
$$+D_3(l_{1x}c_{1y}+a_{1x}m_{1y}-l_{1y}c_{1x}-a_{1y}m_{1x})+D_4(m_{2z}l_{2x}+c_{2z}a_{2x}-l_{2z}m_{2x}-a_{2z}c_{2x})$$
$$+\tfrac{1}{2}K_1(m_{1x}^2+l_{1x}^2+a_{1x}^2+c_{1x}^2)+\tfrac{1}{2}K_2(m_{1y}^2+l_{1y}^2+a_{1y}^2+c_{1y}^2)$$
$$+\tfrac{1}{2}K_3(m_{2x}^2+l_{2x}^2+a_{2x}^2+c_{2x}^2)+\tfrac{1}{2}K_4(m_{2y}^2+l_{2y}^2+a_{2y}^2+c_{2y}^2)$$
$$+K_5(m_{1y}c_{1z}+c_{1y}m_{1z}+l_{1y}a_{1z}+a_{1y}l_{1z})-K_6(m_{1z}l_{1x}+c_{1z}a_{1x}+l_{1z}m_{1x}+a_{1z}c_{1x})$$
$$+K_7(l_{1x}c_{1y}+a_{1x}m_{1y}+l_{1y}c_{1x}+a_{1y}m_{1x})-K_8(l_{2z}m_{2x}+a_{2z}c_{2x}+m_{2z}l_{2x}+c_{2z}a_{2x})-(\mathbf{m}_1+\mathbf{m}_2)\cdot\mathbf{H}\ . \quad (1)$$

We also employ spin-wave-theory restrictions, i.e., $|\mathbf{S}_i|=$ const, which in the base vector designation transform to

$$\begin{aligned}&\mathbf{m}_i^2+\mathbf{l}_i^2+\mathbf{a}_i^2+\mathbf{c}_i^2=\text{ const}\ ,\\ &(\mathbf{m}_i\cdot\mathbf{l}_i)+(\mathbf{a}_i\cdot\mathbf{c}_i)=0\ ,\\ &(\mathbf{m}_i\cdot\mathbf{c}_i)+(\mathbf{l}_i\cdot\mathbf{a}_i)=0\ ,\\ &(\mathbf{m}_i\cdot\mathbf{a}_i)+(\mathbf{l}_i\cdot\mathbf{c}_i)=0\ ,\end{aligned} \quad (2)$$

where $i=1,2$ and in the calculations we must apply Lagrange factor formalism.

The restrictions (2) imposed by the spin-wave-theory approximation are equivalent to the condition of zero parallel susceptibility $\chi_\parallel$ which is valid only at rather low temperatures (much less than T_N). The free-energy term responsible for the parallel susceptibility is of fourth order and consequently, its absence in Eq. (1) is not in contradiction with our approach, which takes into consideration second-order terms only. However, effects resulting from finite $\chi_\parallel$ can be appreciable in certain situations, e.g., at magnetic phase transitions of order-order type or when a magnetic field is applied along the antiferromagnetic axis. The last case will be discussed below in the interpretation of the experimental results.

III. EXPERIMENT

Single-crystal $Ca_2Fe_2O_5$ was grown by a crucibleless zone melting technique which implies remelting and, subsequently, crystallizing a ceramic (pressed and annealed) compound on a seed crystal. Usually this technique is very effective in producing good quality crystals of refractory oxide materials, but dicalcium ferrite turned out to be a rather capricious substance. The procedure had to be repeated several times and each time a small part of the new remelted crystal was used as a seed crystal for the next attempt. Finally, after four such cycles, a good quality single-crystal boule of $Ca_2Fe_2O_5$ was obtained with a cylindrical shape of 40 mm length and 8 mm diameter. The sample used in this investigation was a cube ($3\times3\times3$ mm^3), whose edges were oriented by x-ray diffraction and cut perpendicular to the a,b, and c axes. We have measured the magnetization of this sample in a magnetic field ($-5.5\ \text{T}\le H\le 5.5$ T) using a superconducting quantum interference device (SQUID) magnetometer MPMS (Quantum Design magnetic property measurement system) at temperatures between 5 and 330 K. Figure 4 shows a plot of a magnetization curve with the magnetic field applied along the a axis ($\mathbf{H}\|\mathbf{m}$) at 20 K. It has the regular form typical for an antiferromagnet with a weak ferromagnetic moment. The region of the remagnetization process near zero magnetic field is large enough ($-0.9\ \text{T}\le H\le 0.9$ T) due to a rather small value of the ferromagnetic component ($m_0=0.27$ emu/g at T=20 K) which has been obtained by extrapolation from a large magnetic field ($H\ge 2$ T). The slope of the curve at $H\ge 2$ T is determined by the susceptibility along the a axis ($\chi_a=1.43\times10^{-5}$ cm^3/g at T=20 K). It is interesting to note that the residual magnetization ($H=0$) of the sample is practically zero regardless of the preceding magnetization processes. This effect results from the formation of a domain structure and could serve as a criterion of the crystal quality. Indeed, the intermediate crystals which were used as a seed in the procedure described above have a residual magnetization of one-third of m_0. The strong dependence of the experimental results on crystal quality is perhaps one of the reasons why resolution of the weak ferromagnetism problem in $Ca_2Fe_2O_5$ has dragged on so long.

We should also mention that our results indicating a weak ferromagnetism of intermediate crystals at room temperature ($m_0=10-12\times10^{-2}$ emu/g) agree well with those obtained by Nagata and Ohta[12] ($m_0=7-10\times10^{-2}$ emu/g). However, a crystal of $Ca_2Fe_2O_5$ under investigation has revealed the weak ferromagnetic component value approximately two to three times larger

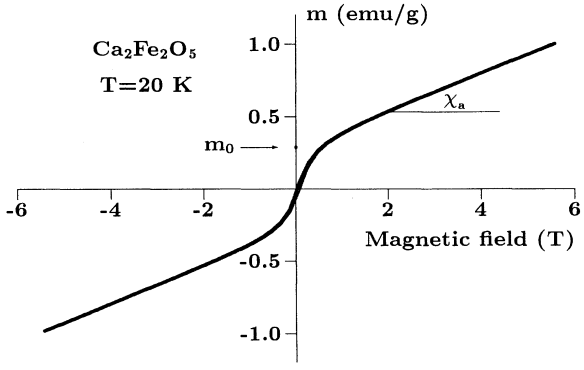

FIG. 4. Magnetization curve of $Ca_2Fe_2O_5$ in a magnetic field applied along the a axis.

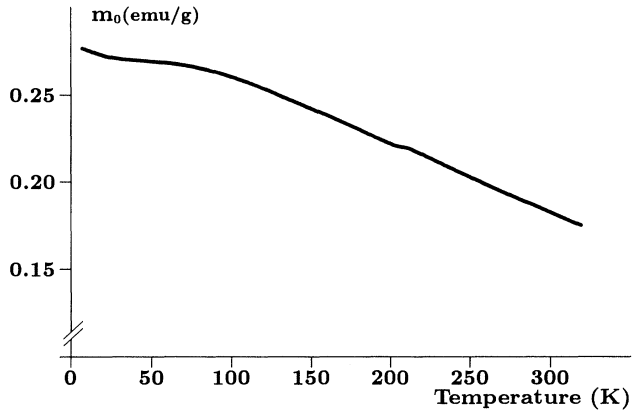

FIG. 5. Temperature dependence of the weak ferromagnetic component in $Ca_2Fe_2O_5$.

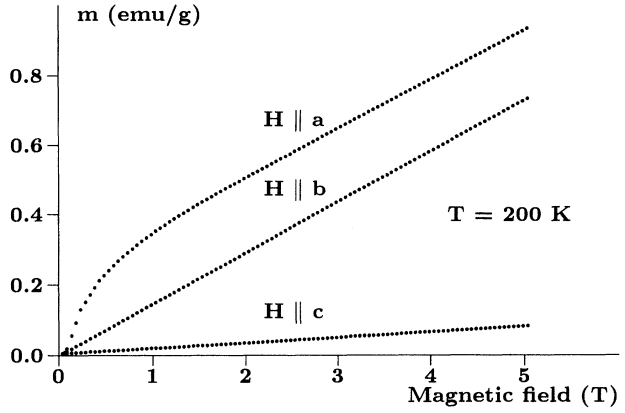

FIG. 7. Typical plot of the magnetization curves in the field applied along the different crystallographic axes for $T=200$ K.

($m_0=20\times10^{-2}$ emu/g, T=300 K) than was observed in Ref. 12.

Magnetization measurements for $\mathbf{H}\|a$ at other temperatures yield a general notion of the behavior of the ferromagnetic component m_0 and susceptibility χ_a. However, there is an easier way to obtain their temperature dependences. It is seen in Fig. 4 that magnetization versus magnetic field, $m(H)$, is a straight line within experimental accuracy for fields larger than 2 T. Therefore, one merely has to measure the magnetization at, for example, 2 and 4 T in order to calculate m_0 and χ_a. Using the temperature dependence of the magnetization at 2 and 4 T, one can obtain m_0(T) (Fig. 5) and χ_a(T) (Fig. 6). Naturally, we have previously made certain, that the magnetization curves at other temperatures (100, 200, and 300 K) have the same form as at 20 K.

Figure 7 shows the magnetization at 200 K in a magnetic field applied along the a,b, and c axes. It is easily seen that the susceptibilities χ_a and χ_b are practically equal for $\mathbf{H}\|a$ and $\mathbf{H}\|b$, i.e., when the magnetic field is perpendicular to the easy axis. Susceptibility along the easy axis χ_c is rather small and increases noticeably with temperature (Fig. 8). The origin of the easy-axis susceptibility will be discussed below.

IV. DISCUSSION

As has been mentioned above, we assume dicalcium ferrite to be primarily a collinear antiferromagnet (l structure, the spins lie along the easy axis) with comparatively small deviations from colinearity and coplanarity due to nonzero components of the **m**, **a**, and **c** vectors. We shall see below that these assumptions are justified by the experimental results. It implies that in the free-energy equation (1), the antisymmetric exchange D_i and anisotropy K_i parameters are essentially smaller than the symmetric exchange interaction B_i parameters. So, in the calculations we shall consider the terms up to the first extent of the ratios D_i/B_j and K_i/B_j. We assume also, that the antiferromagnetic vectors l_1 and l_2 have the same equilibrium values $|l_1|=|l_2|\approx 4M_0$, in accordance with Takeda *et al.*,[9] where M_0 is the atomic magnetic moment. In Ref. 9 $M_0(T)$ was measured by neutron diffraction and turned out to be equal for the two non-

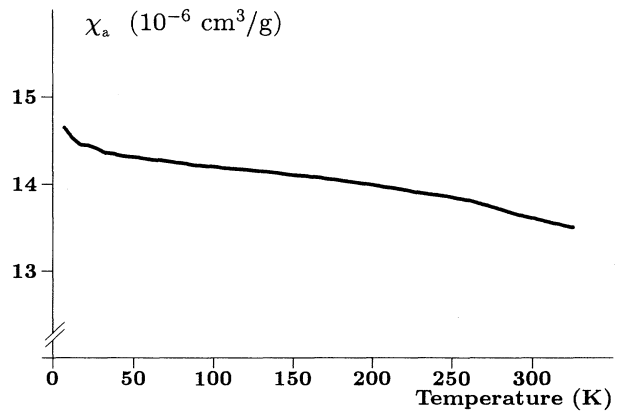

FIG. 6. Susceptibility vs temperature measured along the a axis (orthogonal to the antiferromagnetic vector l).

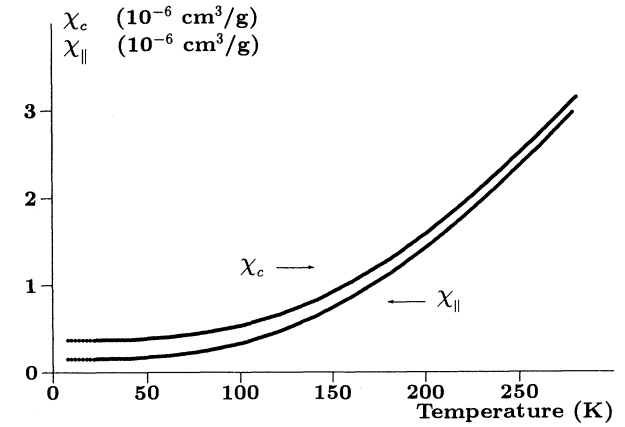

FIG. 8. Easy-axis susceptibility χ_c(T) in comparison with the parallel susceptibility $\chi_\parallel$(T) calculated by Eq. (13).

equivalent positions (4a) and (4c). In the $Pcmn(\Gamma_4^+)$ spin configuration, the nonzero base vectors components are $l_{iz}, m_{ix}(i=1,2)$ and a_{1y} (see Table I). Our model yields $(H=0)$,

$$m_{1x}=\frac{(2B_{2x}+B_3)H_1+B_3H_2}{4B_{1x}B_{2x}+2B_3(B_{1x}+B_{2x})}\ ,$$
$$m_{2x}=-\frac{(2B_{1x}+B_3)H_2+B_3H_1}{4B_{1x}B_{2x}+2B_3(B_{1x}+B_{2x})}\ , \tag{3}$$
$$a_{1y}=\frac{H_3}{B_3+K_2}\ ,$$

where $B_{1x}=B_1+K_1/2, B_{2x}=B_2+K_3/2, H_1=4M_0(D_2+K_6), H_2=4M_0(D_4+K_8)$, and $H_3=4M_0(D_1-K_5)$. The weak ferromagnetic moment is

$$m_0=m_{1x}+m_{2x}=\frac{B_{2x}H_1-B_{1x}H_2}{2B_{1x}B_{2x}+B_3(B_{1x}+B_{2x})}\ . \tag{4}$$

It is well known that there are two mechanisms[14] for weak ferromagnetism in antiferromagnets: (i) antisymmetric exchange interaction and (ii) single-ion anisotropy. Both terms are considered explicitly in the free energy equation (1), where D_i $(i=1,2,3,4)$ corresponds to the former mechanism and K_j $(j=5,6,7,8)$ to the latter. Obviously, the fields H_1 and H_2 in Eq. (4) include both mechanisms. To elucidate the origin of the weak ferromagnetism by means of the magnetization measurements, one needs to measure tensor components which describe the quadratic dependence of the magnetization on the applied field.[19] Unfortunately, this is practically impossible in our case because of the rather small magnitude of this effect. We intend to measure magnetic field frequency dependences of $Ca_2Fe_2O_5$ in the near future in order to clarify the situation with the weak ferromagnetism origin. For the sake of simplicity we shall designate in the following, the two mechanisms as the *effective* Dzyaloshinskiy-Moriya interaction.

The layer structure of $Ca_2Fe_2O_5$ provides an interesting possibility for the interpretation of the ferromagnetic component. Indeed, it is reasonable to propose that the canting in each layer has a common cause. Then, in the framework of this assumption, the H_1 and H_2 fields, which are responsible for the spontaneous magnetization, should have the same signs. The sign of H_i determines relative directions of the $\mathbf{m}$ and $\mathbf{l}$ vectors. Since the $\mathbf{l}_i$ $(i=1,2)$ vectors are antiparallel because of the antiferromagnetic interaction between the nonequivalent layers, then the ferromagnetic components of the layers $\mathbf{m}_1$ and $\mathbf{m}_2$, should be antiparallel as well. This fact is reflected in Eq. (3) by the different signs for $\mathbf{m}_{1x}$ and $\mathbf{m}_{2x}$ [see also Figs. 3(c) and 3(d)]. It is now clear, that the ferromagnetic vectors $\mathbf{m}_{1x}$ and m_{2x} in the layers could be comparatively large, whereas experimentally we observe a rather small ferromagnetic component due to a compensation effect.

This model could explain the anomalously small weak ferromagnetism of $Ca_2Fe_2O_5$ in comparison with similar substances. For instance, well-studied rare-earth orthoferrites,[20] which have the same (although without layers) magnetic structure and high Néel temperatures (600–700 K), demonstrate huge (10–20 T) Dzyaloshinskiy-Moriya fields. Unfortunately, magnetization measurements themselves do not permit the H_1 and H_2 fields to be determined separately. We anticipated that this would be possible by means of an interpretation of the field frequency dependences of magnetic excitations (antiferromagnetic resonance) in $Ca_2Fe_2O_5$.

For a magnetic field applied along the a axis $(\mathbf{H}\|x)$ we obtain from Eq. (1):

$$m_x=m_0+\chi_a H\ ,$$
$$\chi_a=\frac{B_{1x}+B_{2x}}{2B_{1x}B_{2x}+B_3(B_{1x}+B_{2x})}\ , \tag{5}$$

with m_0, B_{1x}, and B_{2x} from Eq. (3).

Using Eq. (5) we can rewrite the spontaneous magnetization (4) in the following form:

$$m_0=\chi_a\frac{B_{2x}H_1-B_{1x}H_2}{B_{1x}+B_{2x}}=\chi_a H_d^{\text{eff}}\ . \tag{6}$$

Thus, the effective Dzyaloshinskiy-Moriya field is a weighted average of the layer fields H_1 and H_2. The temperature dependence of the field H_d^{eff}, which is responsible for the weak ferromagnetic component and defined by Eq. (6) is shown in Fig. 9.

If a magnetic field is applied along the b axis $(\mathbf{H}\|y)$ the symmetry is changed and in addition to $m_{1x}, a_{1y}, l_{1z}, m_{2x}$, and l_{2z} we also have m_{1y}, a_{1x}, c_{1z}, and m_{2y} components (see Table I). However, two of these new components (a_{1x} and c_{1z}) are proportional to combinations of HD_i/B_j^2 and HK_i/B_j^2, and can be neglected in accordance with our approach. Magnetization along the b axis $(\mathbf{H}\|y)$ has the following form:

$$m_y=m_{1y}+m_{2y}=\chi_b H\ ,$$
$$\chi_b=\frac{B_{1y}+B_{2y}}{2B_{1y}B_{2y}+B_3(B_{1y}+B_{2y})}\ , \tag{7}$$

where $B_{1y}=B_1+K_2/2$ and $B_{2y}=B_2+K_4/2$.

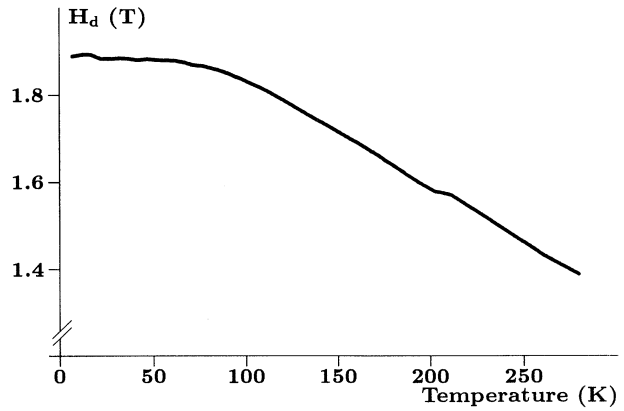

FIG. 9. Temperature dependence of the effective Dzyaloshinskiy-Moriya field for $Ca_2Fe_2O_5$.

The results in Eqs. (5) and (7) can be combined and rewritten as follows:

$$\chi_\alpha^{-1}=B_3+\frac{2B_{1\alpha}B_{2\alpha}}{B_{1\alpha}+B_{2\alpha}} \quad \alpha=x,y \ . \tag{8}$$

We see that the susceptibilities along the a and b axes, (i.e., in a magnetic field applied orthogonal to the easy axis) have the same form and differ only by their anisotropy parameters. On the other hand, our experiments demonstrate an equaility of the χ_a and χ_b susceptibilities:

$$\chi_a=\chi_b=\chi_\perp \ . \tag{9}$$

This is possible if the system is sufficiently isotropic ($K_1\approx K_2, K_3\approx K_4$) or if the anisotropy fields are small compared to the exchange fields. An effective exchange field can be calculated according to the formula,

$$H_E^{\text{eff}}=\chi_\perp^{-1}\tilde{M}_0=8M_0(\chi_\perp\rho V_e)^{-1} \ , \tag{10}$$

where $\tilde{M}_0$ is the specific magnetic moment (mass magnetization), M_0 the magnetic moment per atom, V_e the volume of the elementary cell of $Ca_2Fe_2O_5$, and ρ the density. The exchange field calculated by means of Eq. (10) is about 1.3×10^3 T and is practically independent of temperature up to 330 K.

To estimate the anisotropy fields we can use the results of Brotzeller *et al.*[21] on the temperature dependences of the magnon modes meausured by Fourier spectrometry. In this work the observed modes were identified with so-called quasiacoustic magnon modes with frequencies proportional to the geometric average of the exchange and anisotropy fields, $\nu\sim(H_E^{\text{eff}}H_A^{\text{eff}})^{1/2}$ (Ref. 13). Thus, an effective anisotropy field in the ac plane is about 0.1 T and in the bc plane about 1 T. We realize that this is only a rough estimate. Nevertheless, it is quite clear that in dicalcium ferrite the anisotropy can be neglected in comparison with the exchange interaction and that the x and y indices in equations for χ_a and χ_b can be omitted.

Let us now consider the susceptibility along the c axis. It is well known[13,22] that applying a magnetic field along the easy axis of an antiferromagnet with weak ferromagnetism induces a reorientation of the spins. An interaction of the field with the ferromagnetic component causes the spins to rotate smoothly from the $\mathbf{S}_i\|\mathbf{H}(Pcm'n')$ state to the $\mathbf{S}_i\perp\mathbf{H}(Pc'mn')$ state. During this rotation, in dicalcium ferrite there are 10 nonzero base vector components (see Table I). Hence, a solution of the equations of state for $H_z\neq0$ has an unacceptable form, since too many parameters would be involved to interpret the experimental results. Moreover, as is shown below, a correct interpretation requires a reduction of the restrictions (2) imposed by spin-wave theory. This obviously makes the calculations more complicated. On the other hand, we have shown in the previous discussion that a description of the experimental results by means of the effective parameters, $H_E^{\text{eff}}, H_d^{\text{eff}}, H_A^{\text{eff}}$, is sufficiently fruitful. It is a direct consequence of the fact that the magnetization measurements yield very few averaged parameters for the substance. Such an approach corresponds to the consideration of the substance as a simple antiferromagnet and permits a preliminary analysis of the experiment. Following this idea, we shall try qualitatively to understand the origin of the easy-axis susceptibility. All the parameters mentioned below are implied to be effective parameters, so we omit "eff" everywhere.

The common form of the easy-axis susceptibility for an antiferromagnet with a weak ferromagnetic component is[13]

$$\chi_c=\chi_\perp\frac{H_d^2}{H_EH_A} \ . \tag{11}$$

The formula (11) is valid for small fields compared to the transition field H_{tr}, at which the spin reorientation completes[22]:

$$H_{\text{tr}}=-H_d/2+\sqrt{H_d^2/4+H_EH_A} \ . \tag{12}$$

Using Eq. (11) one can determine the value for H_EH_A to be 30 T^2 ($\chi_c, \chi_\perp$, and H_d are known from our experiments) and then estimate by means of Eq. (12) the transition field H_{tr} which turns out to be about 4.5 T. In accordance with the estimation we should observe a full picture of the spin reorientation in the magnetic field applied along the easy axis (as for instance, in Ref. 23). Nevertheless, it is quite clear from Fig. 7 that we are still rather far from the spin reorientation completion.

We propose that this discrepancy is a result of an interpretation of the experiments in the framework of classical spin-wave theory which assumes that all spin values are constant. As mentioned above, this restriction is justified for low temperatures. However, for a noncontradictory description of the experiments at higher temperatures we must refuse this restriction. In such an approach, the easy-axis susceptibility consists of two terms:

$$\chi_c=\chi_\parallel+\chi_\perp\frac{H_d^2}{H_EH_A} \ . \tag{13}$$

The first term in Eq. (13) is the actual parallel susceptibility, i.e., the response of the sublattice magnetizations to the parallel applied magnetic field, and the second term is the usual rotational part (11) resulting from the presence of the weak ferromagnetic component. The magnetization measurements themselves do not allow a separate determination of these two terms, since the value of H_EH_A is unknown. However, as has been mentioned above, the geometric average of the exchange and anisotropy fields determines the frequency of one of the antiferromagnetic resonance modes which has been measured in Ref. 21. Using these data we can calculate the parallel susceptibility $\chi_\parallel$ separately. Figure 8 shows the temperature dependence of the $\chi_\parallel$ calculated by means of Eq. (13), compared to the measured χ_c. It is easily seen from this figure that for $T\geq100$ K the parallel susceptibility $\chi_\parallel$ is larger than the rotational term $\chi_\perp H_d^2/H_EH_A$. For $T\geq200$ K the easy-axis susceptibility χ_c is mainly due to the parallel susceptibility $\chi_\parallel$. The other two susceptibilities, χ_a and χ_b, in the weak-field approximation (i.e., $H\ll H_E$), are not affected by $\chi_\parallel$ and all the previous results are valid.

Employing all the experimental and calculated results

we can predict the temperature behavior of the transition field $H_{tr}(T)$ in a second-order term approximation using Eq. (8) which is corrected by the parallel susceptibility (Balbashov *et al.*[24]):

$$H_{tr}=\eta^{-1}(-H_d/2+\sqrt{H_d^2/4+\eta H_E H_A}) , \quad (14)$$

where $\eta=1-\chi_{\parallel}/\chi_{\perp}$.

The transition field $H_{tr}(T)$ calculated from Eq. (14) on the base of the available experimental results is weakly dependent on the temperature in the range 5–330 K. Preliminary experiments on field-induced spin reorientations in $Ca_2Fe_2O_5$ have shown that the experimental value of the H_{tr} ($H_{tr}=14.5$ T at $T=4.2$ K) is in excellent agreement with the predicted value. Thus, in spite of the qualitative character of our analysis, it is suitable for the description of the experimental results.

V. CONCLUSION

We have studied the magnetization of the orthorhombic antiferromagnet dicalcium ferrite in a magnetic field up to 5.5 T applied along the a,b, and c axes of the crystal in the temperature range of 5–330 K. Temperature dependence of the weak ferromagnetic component, the susceptibility perpendicular and parallel to the antiferromagnetic axis, the effective Dzyaloshinskiy-Moriya field, and the exchange field have been determined. The easy-axis susceptibility for $T \geq 100$ K was found to be mainly due to parallel susceptibility which is usually neglected in a spin-wave-theory approximation. The temperature behavior of the transition field (completion of the field-induced spin reorientation) has been predicted.

It was shown on the base of a comprehensive group-theoretical analysis, that the magnetic structure of $Ca_2Fe_2O_5$ can be described by six nonequivalent sublattices. Four of them originate from the Fe(1) ions and form a hedgehog structure (noncoplanar and noncolinear), whereas the Fe(2) ions give rise to the usual antiferromagnetic coplanar two-sublattice structure with equivalent spin pairs. It was found, that the layer structure provides a very interesting possibility for $Ca_2Fe_2O_5$ to be treated as two canted antiferromagnets putting one into another with an *antiferromagnetic* interaction between weak ferromagnetic components. Here the net magnetizations $\mathbf{m}_1$ and $\mathbf{m}_2$ are antiparallel and in the experiments we are only concerned with their difference which is rather small. The phenomenological free energy has been constructed, including all principal terms of second order allowed by symmetry and confined to the most important nearest-neighbor interactions.

The experimental results have been interpreted by means of this free energy. It was shown that the magnetization measurements yield only effective (e.g., similar to a weighted average) parameters, since the number of the corresponding phenomenological constants is more than could be obtained from static experiments. We propose that magnon excitation investigations in $Ca_2Fe_2O_5$ could solve this problem.

ACKNOWLEDGMENTS

One of us, (P.M.), acknowledges the support of the Alexander von Humboldt Foundation. The investigation has been funded by the German Ministry for Research and Technology, under Contract No. 03-Ge2Wue-3. Furthermore, the financial support of the Deutsche Forschungsgemeinschaft is gratefully acknowledged.

*Permanent address: General Physics Institute of the Academy of Sciences, 117942, Moscow, Russia.

[1]E. F. Betraut, P. Blum, and A. Sagnieres, Acta Crystallogr. **12**, 149 (1959).

[2]U. Gonser, R. Grant, H. Wiedersich, and S. Geller, Appl. Phys. Lett. **9**, 18 (1966).

[3]S. Geller, R. Grant, U. Gonser, H. Wiedersich, and G. Espinosa, Phys. Lett. **20**, 115 (1966).

[4]R. Grant, H. Wiedersich, S. Geller, U. Gonser, and G. Espinosa, J. Appl. Phys. **38**, 1455 (1967).

[5]H. Whitefield, Aust. J. Chem. **20**, 859 (1967).

[6]S. Geller, R. Grant, U. Gonser, H. Wiedersich, and G. Espinosa, Phys. Lett. **25A**, 722 (1967).

[7]R. Grant, S. Geller, H. Wiedersich, U. Gonser, and L. Fullmer, J. Appl. Phys. **39**, 1122 (1968).

[8]Z. Fridmann, H. Shaked, and S. Shtrikman, Phys. Lett. **25A**, 9 (1967).

[9]T. Takeda, Y. Yamaguchi, S. Tomiyoshi, M. Fukase, M. Sugimoto, and H. Watanabe, J. Phys. Soc. Jpn. **24**, 446 (1968).

[10]J. C. Grenier, M. Pouchard, and R. Georges, Mat. Res. Bull. **8**, 1413 (1973).

[11]T. Hirone, J. Appl. Phys. **36**, 988 (1965).

[12]Y. Nagata and K. Ohta, in *Proceedings of the International Conference on Ferrites,* Tokyo, Japan, 1980 (Reidel, Dordrecht, 1980), p. 419.

[13]E. Turov and V. Najsh, Sov. J. Met. Metallog. **9**, 10 (1960).

[14]I. E. Dzyaloshinskiy, Zh. Eksp. Teor. Fiz. **32**, 1547 (1957) [Sov. Phys. JETP **5**, 1259 (1957)]; T. Moriya, *Magnetism* (Academic, New York, 1963), Vol. 1.

[15]D. K. Smith, Acta Crystallogr. **15**, 1146 (1962).

[16]*International Tables for Crystallography,* edited by Theo Hahn (Reidel, Dordrecht, 1985), Vol. A, p. 288.

[17]*The Irreducible Representations of Space Group,* edited by J. Zak (Benjamin, New York, 1969).

[18]M. A. Gilleo and S. Geller, Phys. Rev. **110**, 73 (1958).

[19]D. Treves, J. Appl. Phys. **36**, 1033 (1965).

[20]R. L. White, J. Appl. Phys. **40**, 1061 (1969).

[21]C. Brotzeller, R. Geick, P. Marchukov, E. G. Rudashevsky, and A. M. Balbashov, Solid State Commun. **82**, 923, (1992).

[22]K. P. Belov, A. M. Kadomtzeva, and R. Z. Levitin, and Zh. Eksp. Teor. Fiz. **51**, 1306 (1966) [Sov. Phys. JETP **24**, 878 (1967)].

[23]I. S. Jacobs, H. F. Burne, and L. M. Levinson, J. Appl. Phys. **42**, 1631 (1971).

[24]A. M. Balbashov, A. G. Berezin, Yu. M. Gufan, G. S. Kolydko, P. Yu. Marchukov, I. V. Nikolaev, and E. G. Rudashevsky, Pis'ma Zh. Eksp. Teor. Fiz. **41**, 391 (1985) [Sov. Phys. JETP Lett. **41**, 479 (1985)].